Hindawi Publishing Corporation
Journal of Nanomaterials
Volume 2016, Article ID 3439419, 7 pages
http://dx.doi.org/10.1155/2016/3439419

Research Article

Preparation, Characterization, and *In Vitro* and *Vivo* Antitumor Activity of Oridonin-Conjugated Multiwalled Carbon Nanotubes Functionalized with Carboxylic Group

Chuanjin Wang and Wei Li

Department of Pharmaceutical Engineering, Institute of Chemical Engineering, Nanjing University of Science and Technology, Nanjing 210094, China

Correspondence should be addressed to Chuanjin Wang; wangchuanjin302@sohu.com

Received 5 December 2015; Revised 18 April 2016; Accepted 26 July 2016

Academic Editor: Ester Vazquez

Carbon nanotubes have shown great potential in tumor therapy. Oridonin (ORI) is a poorly water-soluble diterpenoid compound ($C_{20}H_{28}O_6$) used in the treatment of esophageal and hepatic carcinoma for decades. For the purpose of enhancing the antitumor potency and reducing cytotoxicity of ORI, multiwalled carbon nanotubes functionalized with carboxylic group (MWCNTs-COOH) were used as ORI carrier. ORI was noncovalently encapsulated into (or onto) the functionalized carbon nanotubes (MWCNTs-ORI). The obtained MWCNTs-ORI has been characterized. The ORI loading efficiency in MWCNTs-COOH carrier was studied to be about 82.6% (w/w). *In vitro* cytotoxicity assay on MWCNTs-ORI gave IC_{50} of 7.29 ± 0.5 μg/mL and ORI-F gave IC_{50} of 14.5±1.4 μg/mL. The antitumor effect studies *in vivo* showed that MWCNTs-ORI improved antitumor activity of ORI in comparison with ORI-F. The tumor inhibition ratio for MWCNTs-ORI (1.68×10^{-2} g·Kg^{-1}·d^{-1}) was 86.4%, higher than that of ORI-F (1.68×10^{-2} g·Kg^{-1}·d^{-1}) which was 39.2%. This can greatly improve the pharmaceutical efficiency and reduce potential side effects.

1. Introduction

ORI (Figure 1) is the major active constituent extracted from *R. rubescens* [1]. More than half a century ago, ORI was shown to have a variety of biological effects such as immunoregulatory and anti-inflammatory functions as well as antiviral functions, especially in upper respiratory tract infection. Recent laboratory and clinical data suggest that ORI is a very effective antitumor agent with profound effects on a number of malignant diseases such as prostate, breast, and nonsmall cell lung cancers [2–4]. It has been considered to be potential new cancer chemoprevention agents [5]. However, ORI is unstable and insoluble. Its biological half-life is short. Its therapeutic index is low. This has limited the clinical application of the chemotherapy medicine. The development of a suitable carrier system for ORI will play a quite important role in its preferable application.

Carbon nanotubes (CNTs) are hollow structure and nanodiameter (diameter ~1–100 nm), which are classified into three groups: (1) SWCNTs (single-walled), (2) DWCNTs (double-walled), and (3) MWCNTs (multiwalled). CNTs have received a great interest in a highly efficient delivery vehicle for drugs due to their unique physicochemical properties such as high young modulus, high thermal conductivity, and large surface area [6, 7]. However, CNTs produced initially are insoluble and less dispersible substances. It becomes essential that the hydrophilic groups are introduced onto the hydrophobic surface of CNTs to improve their surface properties for enhanced dispersion, solubilization, biocompatibility, and reduced cytotoxicity [8]. Tan et al. formulated betulinic acid (a poorly water-soluble drug) in MWCNTs-COOH to improve delivery efficiency into cancer cells while reducing cytotoxicity [9].

In this paper, MWCNTs-COOH was used as ORI vehicle at a very high loading efficiency for efficient delivery by π-π stacking [10]. In this research, we report on the characterization of novel drug system (MWCNTs-ORI) by Fourier transform infrared (FTIR), thermogravimetric analysis (TGA), and field emission scanning electron microscopy (FESEM) techniques and investigate their release profiles. In addition,

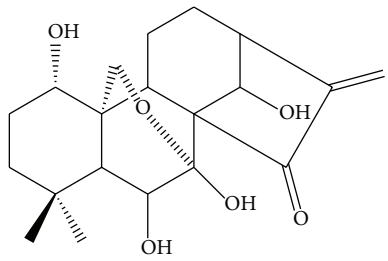

Figure 1: Chemical structure of oridonin.

cell cytotoxicity properties of MWCNTs-ORI were evaluated using the cell counting kit-8 (CCK-8) assay in human liver cancer cells (HepG-2). Finally, the antitumor effect *in vivo* of MWCNTs-ORI was compared to that of ORI-F in murine HepG-2 tumor-bearing mice.

2. Materials and Methods

The herb of *Rabdosia Rubescens* Hemsl was collected in Jiyuan, Henan Province, China. ORI (purity: 99.0%) was isolated from *Rabdosia rubescens* Hemsl in laboratory as previously described [11]. Briefly, *Rabdosia rubescens* Hemsl (160 g) was obtained as the complete dried plant and then ground to powder with particle size less than 0.30 mm and was ultrasonically extracted three times with 95% ethanol for 30 minutes each time. The filtrates were combined and ultrasonically decolored two times for 15 mins with 38.4 g of activated carbon each time. The combined filtrates were dried under reduced pressure and the residue was dissolved in 10 mL of methanol. This solution was then filtered through a 0.22 μm micropore membrane and was injected into the HPLC instrument for separation of ORI. The preparative chromatography conditions were as follows: waters 600 controller; a waters 600 pump; a waters 2487 UV detector; μ Bondapak TM C_{18} column (80 mm id × 300 mm, grain size 25~40 μm); column temperature: 40°C; mobile phase (methanol : water, 50 : 50, v/v); flow rate (60 mL/min); detection wavelength (239 nm); and injection volume (10 mL). The fraction eluting in the range of 16 min~23 min was collected, evaporated, and vacuum dried. About 0.5 G white powder of ORI was obtained.

MWNTs-COOH was purchased from Beijing Dk Nano Technology Co., Ltd. (external diameter 50 nm, purity > 98%, length 10–20 μm, specific surface area > 40 $m^2 \cdot g^{-1}$, bulk density 0.185–7 $mL \cdot g^{-1}$, and -COOH 0.43 wt%). HepG-2 cells were provided by the Nanjing University of Traditional Chinese Medicine Immunization Center. Male BALB/c nude mice were purchased from the Nanjing University of Traditional Chinese Medicine Experimental Animal Center. The animal experimentation was performed in accordance with the Guidelines for Animal Experimentation of the University. EnoGeneCell™ counting kit-8 (CCK-8) was supplied by Nanjing EnoGene Biotech. Co., Ltd. 96-well culture plates were purchased from Costar Corporation. RPMI-1640 medium (Gibco Corporation) containing 10% heat-inactivated newborn calf serum (Hangzhou Sijiqing Biotech Co., Ltd.), 100 $IUmL^{-1}$ penicillin, and 100 $\mu g \cdot mL^{-1}$ were obtained from AMRESCO. Taxol injections were supplied by Sichuan Nanchong Pharmaceutical. Co., Ltd., Taiji Group. Phosphate buffered saline (PBS, containing 1.56 $g \cdot L^{-1}$ $Na_2HPO_4 \cdot H_2O$ + 0.2 $g \cdot L^{-1}$ KH_2PO_4 + 0.2 $g \cdot L^{-1}$ KCl + 8.0 $g \cdot L^{-1}$ NaCl, pH 7.4) was used in the experiments. Dulbecco's Modified Eagle's Medium (DMEM) and fetal calf serum were purchased from Life Technologies (Rockville, Maryland). HPLC grade methanol (Fisher, Loughborough, UK) and ultrapure water were used for all analyses. The methanol and ethyl alcohol for plant extraction were of AR grade purchased from Nanjing Chemical Corporation (Nanjing, China). All other chemicals were of analytical grade.

2.1. Instruments and Measure. To determine the drug loading and release, the content of ORI was quantified by HPLC (Waters 515, USA). Fourier transform infrared (FTIR) spectroscopy was carried out on an FTIR spectrometer (Thermo Scientific Nicolet IS10, USA). To determine the actual drug loading, TGA was performed using a TGA/SDTA851e (TA Instruments, New Castle, DE, USA) with a heating rate of 10°C/min, from room temperature to 800°C, under a nitrogen atmosphere (nitrogen flow rate 40 mL/min). The drug content was determined from the weight loss between 50°C and 800°C. The surface images of these samples were obtained with field emission scanning electron microscopes (JEOLJSM-6380LV, Japan) and transmission electron microscopy (TEM, JEM-2010HR, Japan JEOL). The cytotoxicity of MWCNTs-ORI and ORI-F to HepG-2 was assessed by CCK-8 assay.

2.2. Preparation of MWCNTs-ORI. Briefly, ORI loading was performed by simply mixing ORI (0.3 $mg \cdot mL^{-1}$) with the MWCNTs-COOH dispersions (0.5 $mg \cdot mL^{-1}$) in phosphate buffered saline (PBS) at pH 7.4 and sonicated for 30 minutes at room temperature in an ultrasonic bath. The mixture was then stirred at room temperature to facilitate ORI attachment onto the MWCNTs-COOH. After stirring for 24 hours, the formed complex was centrifuged at 5,000 rpm for 30 minutes, leaving a black precipitate (the product) at the bottom of the centrifuge tube and a clear supernatant, which was retained for further measurement. The product still contained an excessive amount of unreacted (not attached) ORI, which was removed by washing with ethanol and deionized water. After three cycles of washing, centrifuging, and decanting, the product was finally freeze-dried to yield a dry powder of MWCNTs-ORI and stored in a desiccator at 5°C until further characterizations. The amount of unreacted ORI in the supernatant as described was measured by HPLC. HPLC analysis of the ORI was performed with a LiChrospher C_{18} column (4.6 mm id × 250 mm, grain size 5 μm). The mobile phase was methanol and water (70 : 30, v/v). The injection volume was 10 μL. The flow rate was 1.0 mL/min. Column temperature was maintained at 40°C, and the UV detector wavelength was set at 239 nm. The loading of ORI in MWCNTs-COOH was calculated by the following equation:

$$\text{Drug loading\%} = \frac{(W_{\text{total}} - W_{\text{free}})}{W_{\text{total}}} \times 100\%. \quad (1)$$

W_{free} is the analyzed weight of free drug in the supernatant; W_{total} is the analyzed weight of ORI used in formulation.

All data were averaged from three measurements.

2.3. Cell Culture. HepG-2 cells were maintained in DMEM supplemented with 10% FCS, 4.5 mg/mL glucose, 2 mM glutamine, 100 U/mL penicillin G, and 100 mg/mL streptomycin.

2.4. In Vitro Cytotoxicity Testing. Cytotoxicity of MWCNTs-ORI, MWNTs-COOH, and ORI was determined by the CCK-8 assay, as described previously [12]. Briefly, cells were counted, transferred into 96-well microtiter plates, and incubated for 24 h prior to the addition of test compounds. Compound (MWNTs-ORI, MWNTs-COOH or ORI) was dissolved in DMSO and diluted in sterile media, as necessary, to obtain the appropriate concentration. Exponentially growing cells of HepG-2 were made into single-cell suspensions with 0.25% trypsin, at a cell concentration of 1×10^5/mL. 90 μL cells (9×10^3) were seeded into each well of a 96-well plate. HepG-2 cells were incubated for 24 h before they were treated with MWCNTs-ORI, MWNTs-COOH, and ORI which were in a medium containing 0.1% DMSO, which showed no inhibitory effect on cell growth. This experiment was performed using 8 different final drug concentrations (1.875, 3.750, 6.250, 12.500, 25.000, 50.000, 100.000, and 200.000 μg/mL). To each well was added 10 μL of the appropriate drug. Control cells were treated with an equal volume of serum-free RPMI-1640 containing 0.1% DMSO. The volume of DMSO added to each well was no more than 1×10^{-2} μL. After cells had been cultured for 48 h, 10 μL CCK-8 was added to each well. One hour later, the cell viability ratio was determined from the absorbance measured at 450 nm.

Each sample was assayed in triplicate, and each assay was repeated twice. Results are expressed as the concentration yielding 50% inhibition (IC_{50}):

$$\text{The inhibition rate (\%)} = \left[\frac{\left(A_{\text{control}} - A_{\text{experiment}}\right)}{A_{\text{control}}}\right] \times 100\%. \quad (2)$$

Data were expressed as mean ± SD. One-way analyses of variances and Fisher's least significant difference were performed using SAS 8.13. Differences were significant at $^*P < 0.05$.

2.5. Evaluation of In Vivo Antitumor Activity. Tumor-bearing mice were prepared by inoculating a suspension of HepG-2 cells (1.2×10^6 cells resuspended in 200 μL of 0.9% physiological saline) subcutaneously into the right armpit of each of the male BALB/c nude mice (age 5–7 weeks, body weight 20.25 ± 2.34 g). On day 5 after inoculation, the tumors were about approximately 100 mm^3, and 40 mice were randomly assigned to 4 treatment groups (10 mice per group): MWCNTs-ORI suspended in isotonic saline (ORI: 1.5×10^{-2} g·Kg^{-1}·d^{-1}), ORI-F suspended in isotonic saline (1.5×10^{-2} g·Kg^{-1}·d^{-1}), and MWCNTs-COOH suspended in isotonic saline (without ORI) and isotonic saline (negative control). Mice were given an intravenous injection via the tail vein for 10 days.

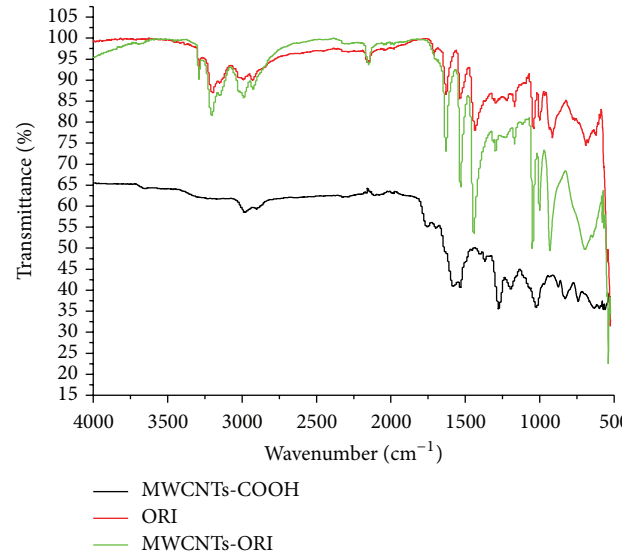

Figure 2: Fourier transform infrared spectroscopy of MWCNTs-COOH before and after loading with ORI.

The tumor volumes were measured with caliper measurements every other day and calculated using the formula tumor volume = [(tumor width)^2× (tumor length)]/2.

One day after 11, the mice were sacrificed, and the tumors were weighed. The inhibition was calculated as follows: inhibition (%) = $[(A - B)/A] \times 100\%$, where A was the mean tumor weight of the negative control group, and B was that of the ORI-treated or positive-control group.

3. Results and Discussion

3.1. Physicochemical and Characterization of MWCNTs-COOH and ORI Conjugates. The functional groups of MWCNTs-COOH and MWCNTs-ORI were characterized by FTIR. The results clearly demonstrate the FTIR of the MWCNTs-COOH before and after loading with ORI (Figure 2). The absorption peak at 1630 cm^{-1} in the spectra of MWCNTs-ORI could be due to the absorption peak of ORI at 1630 cm^{-1} that could possibly be attributed to the typical stretching band of C=O vibrations of carbonyl group. Another absorption peak observed at 1530 cm^{-1} corresponding to the absorption peak of ORI at 1540 cm^{-1} could possibly be attributed to the typical stretching band of C=C vibrations of the vinyl functional group of ORI. In addition, the absorption bands between 2750 and 3375 cm^{-1} were ascribed to the asymmetric and symmetric O-H stretching vibrations from the hydroxyl groups of ORI.

The bands at 2900–3000 cm^{-1} of the MWCNTs-COOH should be due to the asymmetric and symmetric O-H stretching vibrations from the carboxylic group of MWCNT-COOH. The FTIR spectrum of MWCNTs-ORI displays all the characteristic bands of ORI, indicating successful loading of MWCNTs-COOH and ORI. The loading of ORI onto

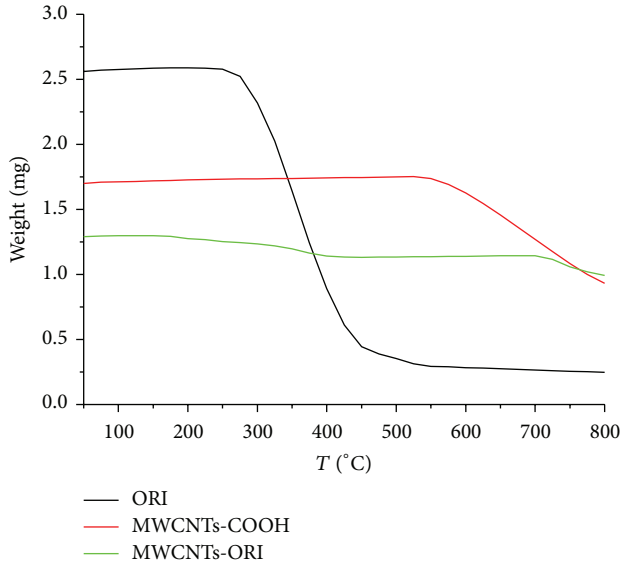

Figure 3: Thermogravimetric analysis profiles of ORI, MWCNTs-COOH, and MWCNTs-ORI.

MWCNTs-COOH could be attributed to simple π-π stacking and hydrophobic interactions.

Different thermal decay profiles point to structurally different materials. The thermal decomposition profiles were obtained under a steady flow of N_2, at a heating rate of $10^{\circ}C \cdot min^{-1}$ as shown in Figure 3. Any H_2O solvent could not be seen released from the ORI and MWCNTs-ORI starting around 100°C. These values illustrated less water contained onto the ORI and MWCNTs-ORI. The decomposition of Ph started at about 270°C. The carbon skeleton of MWCNTs-COOH started to decompose from 550°C. The thermal degradation of MWCNTs-ORI was a multistep process. The first weight losses occurred in the range of (50~250°C) assigned to the elimination of surface physisorbed water. The weight loss region (250~550°C) could be due to the decomposition of ORI. The third stage (700~800°C) could be explained by the initial decomposition of MWCNTs-COOH. An important observation was that the decomposition of MWCNTs-COOH began at about 550°C, whereas in the MWCNTs-Ph it started at about 700°C. The higher thermal stability of MWCNTs-ORI could be attributed to ORI molecules adsorbed onto the sidewalls of MWCNTs-COOH. The thermogravimetric analysis showed a weight loss of 90.3% for ORI, 45.2% for MWCNTs-COOH, and 23.0% for MWCNTs-ORI at 800°C. MWCNTs-ORI exhibited a higher thermal stability compared to MWCNTs-COOH and ORI. These results could be attributed to the fact that ORI molecules could be grafted onto the surface of MWCNTs-COOH through π-π stacking and H-bonding interactions.

3.2. Electron Microscopy. Field emission scanning electron microscope (FESEM) was used to characterize the MWCNTs-COOH (Figure 4(a)) and MWCNT-ORI (Figure 4(b)). Figure 4(a) showed the typical image of the commercially obtained MWCNTs-COOH with a smooth surface in an agglomerated state. Following the drug loading process (Figure 4(b)), the MWCNT-ORI had a granular surface in a more dispersed form. This indicates that the surface of MWCNTs-COOH was coated with ORI. Different sizes are observed due to MWCNTs-COOH overlapping on each other, which could be as a result of aggregation.

Table 1: IC_{50} values of various formulations of ORI on HepG-2 cells.

Formulation	IC_{50} (μg/mL)
ORI-F	14.50 ± 1.40
MWCNTs-ORI	7.29 ± 0.50
MWCNTs-COOH	54.40 ± 3.70

IC_{50} is defined as the concentration that resulted in a 50% decrease in cell number and the results are means ± standard deviation of three independent replicates.

The transmission electron microscopy (TEM) was also applied to characterize the MWCNTs-COOH (Figure 4(a)) and MWCNT-ORI (Figure 5(b)) to get a higher magnification of TEM images. MWCNTs-COOH and MWCNT-ORI were negatively stained with 1% phosphotungstic acid for 60 s. Figure 5(a) shows an image of the commercially attained MWCNTs-COOH with smooth surfaces. Following the drug loading technique (Figure 5(b)), the MWCNT-ORI had uneven surface. The diameter of MWCNTs-COOH carbon after loading ORI was enhanced. These results showed that the ORI was loaded to the surface of MWCNTs-COOH.

3.3. ORI Loading. The commonly used anticancer drug, ORI, has a conjugate plane structure and the structure of MWNTs can be visualized by rolling up a graphite sheet to a tube. The possible interaction of ORI noncovalently attached to MWCNTs-COOH via π-π stacking and hydrogen bond between -OH and -COOH groups. The loading of ORI in MWCNTs-COOH was determined by HPLC. After the centrifuge separation, the supernatant was collected and then measured at 239 nm, which is the characteristic absorption for ORI. By comparing peak area of the unreacted ORI in the supernatant with the original ORI solution, the loading of ORI was calculated to be around 82.6%.

3.4. In Vitro Cytotoxicity Testing. In order to evaluate the anticancer activity of MWCNTs-ORI, MWCNTs-COOH and ORI-F *in vitro* cytotoxicity studies were also performed on HepG-2 cells using CCK-8 assays, as shown in Figure 6 and Table 1. It was observed that MWCNTs-ORI demonstrated significant cell growth inhibitory to HepG-2 cells in a concentration-dependent manner. The IC_{50} of MWCNTs-ORI in HepG-2 cell lines was 7.29 μg/mL; this value was far below that of ORI-F (IC_{50} = 14.5 μg/mL). Cellular and molecular mechanisms were known that the main advantage of CNTs is that their structure enhances direct uptake through cellular membrane without any detrimental effect on the biological functionality of the cell [13]. On the other hand, MWCNTs-COOH also exhibited significant cytotoxicity on HepG-2 cells. However, an amount 40 μg/mL of oxidized MWCNTs could be utilized for a CNT drug delivery system in nanomedicine indicating that MWCNTs-COOH

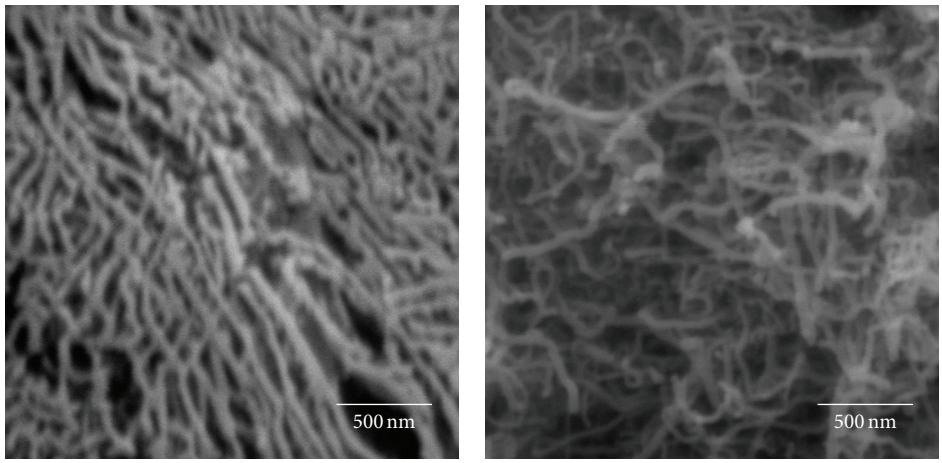

(a) (b)

Figure 4: FESEM photographs of MWCNTs-COOH (a) and MWCNT-ORI (b).

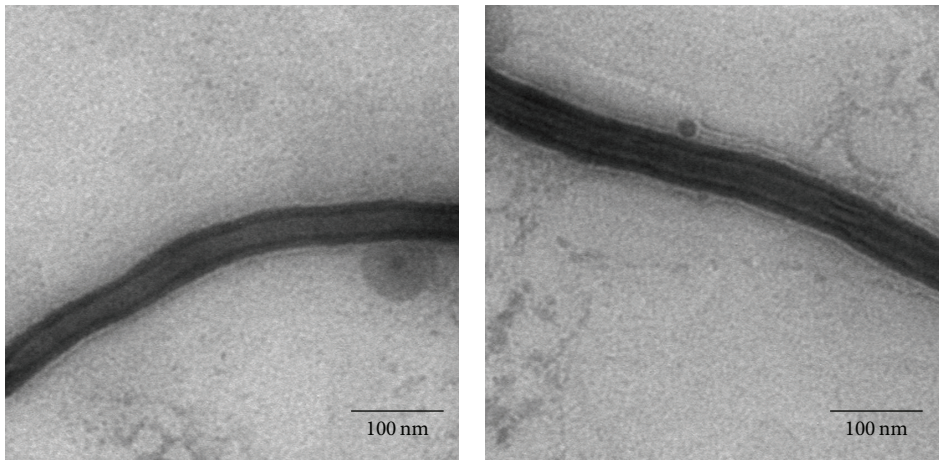

(a) (b)

Figure 5: TEM photographs of MWCNTs-ORI (a) and MWCNTs-COOH (b).

has a relatively good biocompatibility [14]. Other researchers also reported an MWCNT formulation for the delivery of betulinic acid (BA) with enhanced delivery efficiency into cancer cells by using a simple preparation method. It was shown that MWCNT-BA demonstrated moderate cell growth inhibitory activity to HepG-2 in a concentration-dependent manner. The IC_{50} of MWCNT-BA in HepG-2 cells was 11.0 μg/mL, and this value was below that of free BA (IC_{50} = 15.0 μg/mL) [9]. The results showed that functionalized MWCNT held great potential in the field of nanobiotechnology and nanomedicine.

3.5. Evaluation of In Vivo Antitumor Activity. MWCNTs-ORI, MWCNTs-COOH, and ORI-F were tested for anti-tumor efficacy using the human HepG-2 tumor xenograft model in male BALB/c nude mice. From the beginning of the administration, the tumor volume was measured once every other day for 10 days. The tumor growth curve was plotted. The data of tumor growth curves are shown in Figure 7, which demonstrates very significant tumor growth inhibition in response to treatment with MWCNTs-ORI compared to other groups. One-way analysis of variance (ANOVA) was performed to demonstrate the difference among the volumes. Tumor-bearing mice treatment with MWCNTs-ORI had about reduction 86% in tumor volume compared with isotonic saline (negative control) group ($P < 0.01$). For isotonic saline group, tumor growth is most evident and maintained a level of rapid growth.

Tumor growth inhibition by MWCNTs-ORI, MWCNTs-COOH, and ORI-F and statistical analysis were shown in Tables 2 and 3. The results presented in Table 2 showed that MWCNTs-ORI (1.48×10^{-2} g·Kg^{-1}·d^{-1}) exhibited very impressive antitumor effect *in vivo* against HepG-2 cells, higher than ORI-F, MWCNTs-COOH, and the negative control group ($P < 0.01$). The tumor inhibition was more than 80%. After 10 days of MWCNTs-ORI treatment, the weight of mice increased.

After the 10-day treatment, MWCNTs-ORI had very significant suppression of tumor growth in transplanted murine HepG-2 cells. Each tumor weight is presented as

Table 2: The effect of various formulations of ORI on the weight of tumor on BALB/c nude mice.

Group	Dose (g/Kg)	Number of animals (start/end)	Body weight (g)		Tumor weight (g)	Tumor inhibition (%)
			Initial	End		
Negative control	—	10/10	19.3 ± 1.3	18.4 ± 1.2	1.22 ± 0.21	
MWCNTs-ORI	1.48×10^{-2}	10/10	19.7 ± 1.5	22.5 ± 0.8	0.17 ± 0.11	86.4
MWCNTs-COOH	1.48×10^{-2}	10/10	20.4 ± 0.9	19.7 ± 1.1	1.08 ± 0.23	11.3
ORI-F	1.48×10^{-2}	10/10	20.8 ± 1.2	20.1 ± 1.3	0.74 ± 0.31	39.2

Table 3: Statistical analysis of the effect of various ORI formulations on the weight of tumor on BALB/c nude mice.

Groups	Negative control	MWCNTs-ORI	MWCNTs-COOH	ORI-F
Negative control		$P < 0.01^{**}$	$P < 0.01^{**}$	$P < 0.01^{**}$
MWCNTs-ORI	$P < 0.01^{**}$		$P < 0.01^{**}$	$P < 0.01^{**}$
MWCNTs-COOH	$P < 0.01^{**}$	$P < 0.01^{**}$		$P < 0.01^{**}$
ORI-F	$P < 0.01^{**}$	$P < 0.01^{**}$	$P < 0.01^{**}$	

$^{**}P < 0.01$ significantly different from various ORI formulations as analyzed by ANOVA.

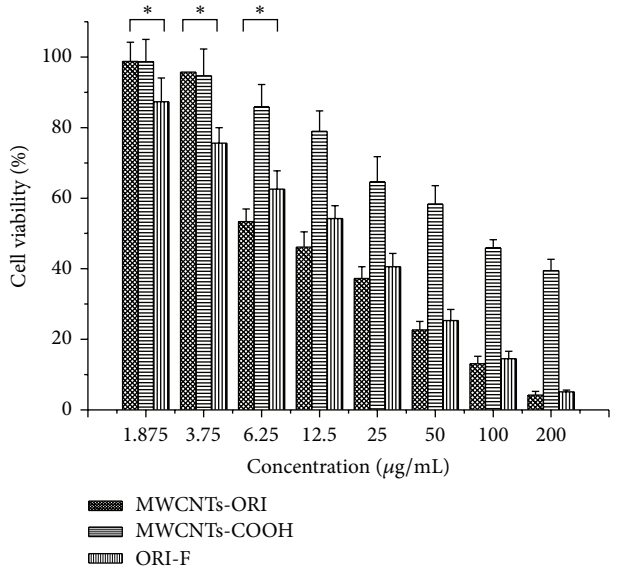

Figure 6: Cell viability of HepG-2 cells treated with MWCNTs-ORI, MWCNTs-COOH, and ORI-F for 48 h. The data presented are mean ± standard deviation of triplicate samples and the difference was considered significant at $^{*}P < 0.05$.

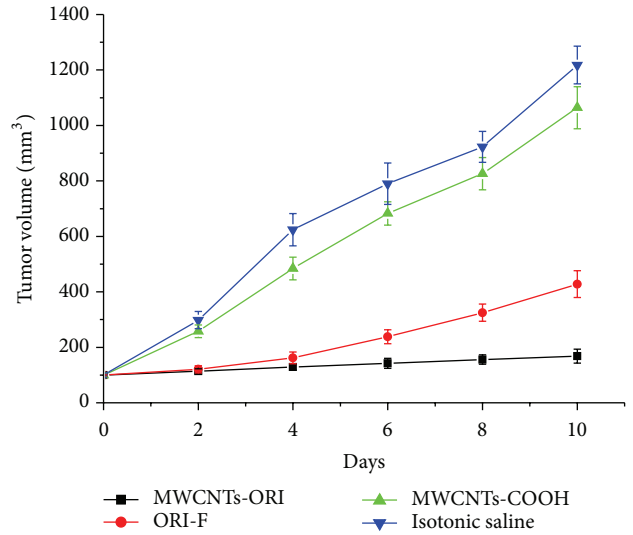

Figure 7: *In vivo* antitumor efficacy of HepG-2 tumor-bearing male BALB/c nude mice treated with isotonic saline (negative control), MWCNTs-COOH, ORI-F, and MWCNTs-ORI ($n = 10$) ($P < 0.01$ by ANOVA with Tukey's post-test).

the mean ± SD. The results of the statistical analysis were shown in Table 3. Tumor growth was suppressed by free ORI-F, MWCNTs-COOH, and MWCNTs-ORI. However, the greatest suppression was observed in the case of MWCNTs-ORI. The above findings indicated that MWCNTs-ORI was more effective than ORI-F in inhibiting tumor growth.

Carbon nanotube-based drug delivery has shown a promise in tumor-targeted accumulation in mice, and the system exhibits good biocompatibility, good excretability, and little toxicity. Various chemotherapeutic reagents have been demonstrated to have increased efficiency after being chemically linked to CNTs [15]. When antitumor reagent 10-hydroxycamptothecin (HCPT) was linked to MWNTs covalently through a cleavable ester linkage using hydrophilic diaminotriethyleneglycol as the spacer between the nanotube and drug moieties, the obtained MWNT-HCPT conjugates were found to be superior to the clinical HCPT formulation in antitumor activity both *in vitro* and *in vivo* [16]. These results indicated that a CNT-based delivery system could be utilized as a delivery of drugs in cancer chemotherapies with improved therapeutic properties.

4. Conclusions

A highly effective DDS based on MWNTs-COOH has been developed in a facile strategy. MWCNTs-ORI was prepared using a simple preparation method. The characterization of the MWCNT-ORI by FTIR and microscopic studies showed

that ORI molecules are loaded on the outer surface of MWCNT-COOH. This indicates that ORI could be attached on the external walls of MWCNT-COOH via π-π stacking interaction due to the strong nonspecific adsorption of CNT, with a 82.6% (w/w) loading of ORI. Cytotoxicity of MWCNTs-ORI was evaluated in HepG-2 cells using CCK-8 assays. It was shown that MWCNTs-ORI had much greater cytotoxicity compared to ORI-F. This indicates that MWCNT-COOH is potentially useful for the delivery of therapeutic agents. The ability of ORI to inhibit tumor also was evaluated. In this study, MWCNTs-ORI exhibited very impressive antitumor effect *in vivo*. In the animal experiments, F-L-ORI (1.48×10^{-2} g·kg^{-1}·d^{-1}) strikingly inhibited HepG-2 cells growth, and the inhibition rate was 86.4%.

In summary, to enhance the anticancer potency of ORI, a novel ligand, MWCNT-COOH, has been used for preparation of MWCNTs-ORI. *In vitro* cytotoxicity and *in vivo* antitumor effect of MWCNTs-ORI were evaluated. The results indicated that this kind of DDS might enhance delivery efficiency into cancer cells. These efforts can potentially lead to the development of MWCNTs-ORI as a clinical agent for the treatment of tumors such as hepatic carcinomas.

Competing Interests

The authors declare that they have no competing interests.

Acknowledgments

The authors are grateful to Nanjing University of Science and Technology. The project was supported by Independent Research Program (Chinese National Scientific Research Training Program-2014).

References

[1] L. C. Meade-Tollin, E. M. K. Wijeratne, D. Cooper et al., "Ponicidin and oridonin are responsible for the antiangiogenic activity of *Rabdosia rubescens*, a constituent of the herbal supplement PC SPES," *Journal of Natural Products*, vol. 67, no. 1, pp. 2–4, 2004.

[2] Q.-B. Han, M.-L. Li, S.-H. Li, Y.-K. Mou, Z.-W. Lin, and H.-D. Sun, "Ent-kaurane diterpenoids from Isodon rubescens var. lushanensis," *Chemical and Pharmaceutical Bulletin*, vol. 51, no. 7, pp. 790–793, 2003.

[3] J.-X. Zhang, Q.-B. Han, A.-H. Zhao, and H.-D. Sun, "Diterpenoids from *Isodon japonica*," *Fitoterapia*, vol. 74, no. 5, pp. 435–438, 2003.

[4] T. Ikezoe, S. S. Chen, X. J. Tong, D. Heber, H. Taguchi, and H. Koeffler, "Oridonin induces growth inhibition and apoptosis of a variety of human cancer cells," *International Journal of Oncology*, vol. 23, no. 4, pp. 1187–1193, 2003.

[5] S. Sheng, N. Bai, and C. S. Yang, "New cancer chemoprevention agents found from herbal medicine and functional food," in *Proceedings of the 227th American Chemical Society National Meeting*, vol. 226, pp. 105–107, Anaheim, Calif, USA, April 2004.

[6] O. Regev, Y. Barenholz, S. Peretz, D. Zucker, and Y. Bavli-Felsen, "Can carbon nanotube-liposome conjugates address the issues associated with carbon nanotubes in drug delivery?" *Future Medicinal Chemistry*, vol. 5, no. 5, pp. 503–505, 2013.

[7] F. Abbaszadeh, O. Moradi, M. Norouzi, and O. Sabzevari, "Improvement single-wall carbon nanotubes (SWCNTs) based on functionalizing with monomers 2-hydroxyethylmethacryate (HEMA) and N-vinylpyrrolidone (NVP) for pharmaceutical applications as cancer therapy," *Journal of Industrial and Engineering Chemistry*, vol. 20, no. 5, pp. 2895–2900, 2014.

[8] S. Vardharajula, S. Z. Ali, P. M. Tiwari et al., "Functionalized carbon nanotubes: biomedical applications," *International Journal of Nanomedicine*, vol. 7, pp. 5361–5374, 2012.

[9] J. M. Tan, G. Karthivashan, P. Arulselvan, S. Fakurazi, and M. Z. Hussein, "Characterization and in vitro studies of the anticancer effect of oxidized carbon nanotubes functionalized with betulinic acid," *Drug Design, Development and Therapy*, vol. 8, pp. 2333–2343, 2014.

[10] N. Nakayama-Ratchford, S. Bangsaruntip, X. Sun, K. Welsher, and H. Dai, "Noncovalent functionalization of carbon nanotubes by fluorescein- polyethylene glycol: supramolecular conjugates with pH-dependent absorbance and fluorescence," *Journal of the American Chemical Society*, vol. 129, no. 9, pp. 2448–2449, 2007.

[11] C. J. Wang, Y. Y. Wei, L. Yu, and L. Zhang, "The effect of stealth liposomes on pharmacokinetics, tissue distribution and antitumor activity of oridonin," *PDA Journal of Pharmaceutical Science and Technology*, vol. 63, no. 5, pp. 409–416, 2009.

[12] Y.-F. Yuan, X.-Y. Hu, Y. He, and J.-G. Deng, "Synthesis and anti-tumor activity evaluation of rhein-aloe emodin hybrid molecule," *Natural Product Communications*, vol. 7, no. 2, pp. 207–210, 2012.

[13] N. W. S. Kam and H. Dai, "Single walled carbon nanotubes for transport and delivery of biological cargos," *Physica Status Solidi (B)*, vol. 243, no. 13, pp. 3561–3566, 2006.

[14] A. Patlolla, B. Knighten, and P. Tchounwou, "Multi-walled carbon nanotubes induce cytotoxicity, genotoxicity and apoptosis in normal human dermal fibroblast cells," *Ethnicity & Disease*, vol. 20, no. 1, pp. S1-65–S1-72, 2010.

[15] H. Y. Xu, J. Meng, and H. Kong, "What are carbon nanotubes' roles in anti-tumor therapies?" *Science China Chemistry*, vol. 53, no. 11, pp. 2250–2256, 2010.

[16] W. Wu, R. Li, X. Bian et al., "Covalently combining carbon nanotubes with anticancer agent: preparation and antitumor activity," *ACS Nano*, vol. 3, no. 9, pp. 2740–2750, 2009.